Identification of clinically relevant spatial phenotypes in large-scale multiplex immunofluorescence data via unsupervised graph learning in non-small cell lung cancer

Abstract #1277

STUDY BACKGROUND

- Multiplex immunofluorescence (mIF[1]) allows simultaneous spatial interrogation of multiple cell- and tissue-based biomarkers from patient cohorts at scale using whole-slide images (WSI).
- The study of the spatial relationships between cells is of increasing importance in immuno-oncology. For instance, spatial analyses could inform the effects of a cancer treatment on the tumor immune microenvironment. However, the identification of spatially-derived insights is limited by conventional approaches that reduce spatial data into human-derived feature sets (e.g., nearest neighbor), necessitating new methods for surveying spatial patterns in full.
- We hypothesize that an unsupervised approach to mIF analysis using graph neural networks (GNN) will allow identification of 'spatial phenotypes' defined by their cellular composition and spatial arrangement in clinical datasets. Here, we identify clinically-relevant, interpretable spatial phenotypes with distinct immunogenic profiles in non-small cell lung cancer (NSCLC).

MULTIPLEX IMMUNOFLUORESCENCE

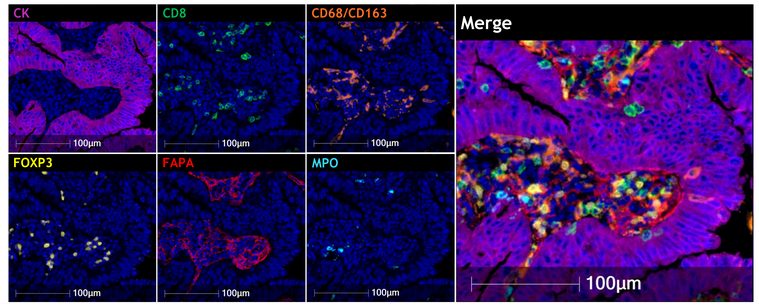

Figure 1. Example multiplex immunofluorescence from an NSCLC case. Individual channels and a merged overlay are depicted. Fluorophores used are as follows: CK: Opal690, CD8: Opal480, CD68/CD163: Opal780, FOXP3: Opal570, FAPA: Opal 620; MPO: Opal520, Nuclei: DAPI.

METHODS

Patient samples and immunofluorescence.

- Formalin-fixed, paraffin-embedded clinical NSCLC samples (N=165 from 150 cases) were obtained from commercial sources (**Table 1**). To identify relevant cancer, stromal, and immune cell types, we stained cytokeratin (CK), CD8, FoxP3, myeloperoxidase (MPO), CD68/CD163, and fibroblast activation protein-A (FAPA) while labeling all nuclei with DAPI (**Fig. 1**). mIF images were acquired and spectrally unmixed using the Phenoptic platform (Akoya) and HALO-AI software (Indica Labs).
- From the same cohort, bulk mRNAseq and proteomic analyses were performed.

Table 1. Cohort characteristics.

Characteristic	N
Sample Site	
Primary	115
Distant Metastasis	50
Histological Subtype	
Adenocarcinoma	115
Squamous Cell Carcinoma	44
Other	6
Treatment History	
Naïve	111
Recent chemotherapy (<100 days)	24
Previous chemotherapy (>100 days)	15

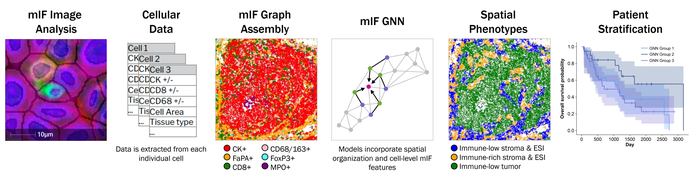

Figure 2. Study workflow. From left to right: Cells are segmented from images and used for graph construction. An unsupervised GNN learned to identify characteristic spatial phenotypes defined by these features and the spatial arrangement of cells. Finally, relative spatial phenotype abundance was used to stratify patients into groups.

Unsupervised exploration of tissue organization and statistical analysis.

- The overall study workflow is shown in **Fig. 2**.
- A convolutional neural network was trained to segment regions of cancer epithelium, stroma, and necrosis, while a pretrained network segmented all cells (HALO-AI). Cells were converted into graphs with 12 node features related to cell phenotypes, tissue types, nuclear morphology, and undirected edges were constructed from each node with its five nearest neighbors.
- A GNN autoencoder[2] was trained to discover tissue patterns defined by spatial arrangement and mIF cell/tissue phenotypes. Inspection of latent GNN node representations revealed three distinct groups, termed spatial phenotypes, which were clustered using k-means (**Fig. 3**).
- Hierarchical clustering identified patient subsets based on these patterns, and Cox proportional hazard models assessed overall survival (OS).

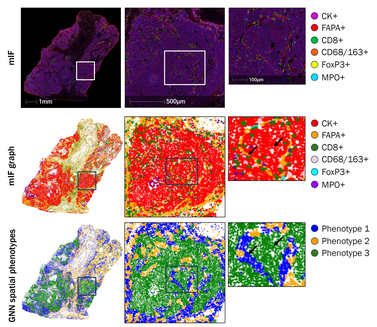

Figure 3. GNN-based identification of spatial phenotypes in NSCLC. Example mIF images (top), mIF graph rendering (middle) and GNN spatial phenotypes (bottom) identified in an NSCLC specimen. Spatial phenotypes capture both the composition and spatial organization of cellular neighborhoods.

RESULTS

Figure 4. GNN-derived spatial phenotypes are interpretable and have clinical value in NSCLC.

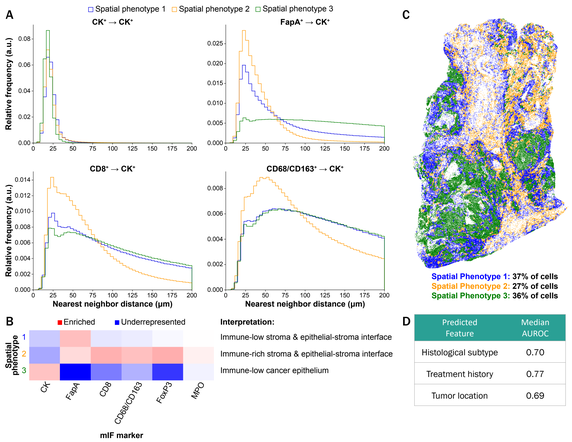

Predicted Feature	Median AUROC
Histological subtype	0.70
Treatment history	0.77
Tumor location	0.69

- Spatial relationships (here: nearest neighbor distances) captured by GNN classification are shown in panel A. Fibroblasts and epithelial cells are in close range in spatial phenotypes 1&2, while immune cells in spatial phenotype 2 are located more proximal to epithelial cells.
- GNN-derived spatial phenotypes showed unique cell type enrichment patterns.
- Example rendering of spatial phenotypes in a NSCLC clinical specimen, with quantified frequencies of each is shown in panel C.
- GNN-derived spatial phenotypes can predict clinical features in NSCLC (D).

Figure 5. Patient stratification based on GNN tissue phenotypes shows interpretable differences in gene expression.

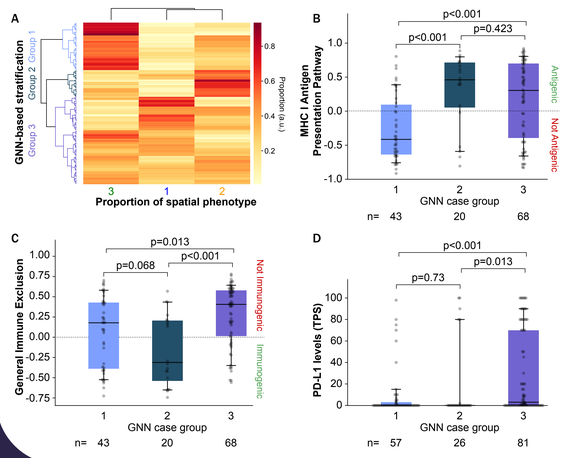

- Unsupervised hierarchical clustering based on GNN-derived spatial phenotypes identifies distinct patient groupings (A).
- A custom-derived MHC I antigen presentation pathway gene expression signature (HLA-A, HLA-B, HLA-C, TAP1, TAP2, NLRC5, B2M, TAPBP, PSMB8, PSMB9, and PDIA3) and a previously published general immune exclusion gene expression signature[3] were assessed. MHC I antigen presentation (B) and general immune exclusion signatures (C) differed between GNN case groups.
- Manual PD-L1 scoring (TPS) corresponds to relative antigenicity and immunogenicity determined by gene expression analysis (D).

Figure 6. Prognostic differences between GNN case groups in mostly treatment naïve NSCLC patients.

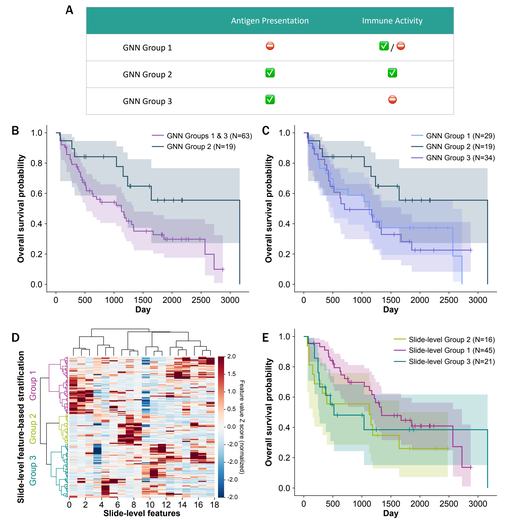

- GNN-derived groups have significant prognostic differences. A summary of antigenicity and immunogenicity of GNN case groups is shown in panel A.
- Patients in GNN group 2 (high antigenicity, immunogenicity) show improved OS compared to patients in groups 1 and 3 (B; p=0.04), but not in a three-way comparison (C; p=0.08).
- Unsupervised hierarchical clustering based on slide-level mIF features (e.g., phenotype proportion features) identifies distinct slide-level groupings (D) which do not show meaningful differences in OS (E).

CONCLUSIONS

We developed a novel, unsupervised deep-learning-based GNN for analysis of WSI mIF data in NSCLC. This method identified interpretable tissue phenotypes with clinically-relevant differences in anti-tumor immunity and prognosis. These data show the utility of unsupervised spatial deep-learning methods, compared to traditional approaches, for data-driven discovery of complex patterns in large-scale multiplex images.

AUTHORS

Robert Egger[1*], Andrew Fisher[2*], Michael G. Drage[1], Jimena Trillo-Tinoco[2], John Abel[1], Andrew Browne[2], Deepta Rajan[1], Tai Wang[2], Jake Conway[1], Catherine King[2], Jacqueline Brosnan-Cashman[1], Sergine Brutus[1], Anne Lewin[2], Arnaud Amzallag[2], Thomas Lila[2], Tyler Simpson[2], Mike Montalto[1], Benjamin Chen[2], Ben Glass[1^], Vipul Baxi[2^]

*Primary authors
^Corresponding authors

[1] PathAI, Boston, MA
[2] Bristol Myers Squibb, Cambridge, MA

CONTACT

Robert Egger: robert.egger@pathai.com
Andrew Fisher: andrew.fisher@bms.com

REFERENCES

1. Gerdes, M.J. *et al. Proc Natl Acad Sci USA.* 2013; **110**(29):11982-11987.

2. Kipf, T.N., Welling, M. 2016; arXiv:1611.07308.

3. Jerby-Arnon, L. *et al. Cell.* 2018; **175**(4):984-997.

ACKNOWLEDGMENTS

We thank Bioscience Communications for assistance with figure design.

This work was funded by PathAI and Bristol Myers Squibb.

This poster template was developed by SciStories LLC. https://scistories.com/